Electrospinning Fabrication of High Strength and Toughness Polyimide Nanofiber Membranes Containing Multiwalled Carbon Nanotubes

Dan Chen,[†] Tianxi Liu,*[,†] Xiaoping Zhou,[§] Wuiwui Chauhari Tjiu,[‡] and Haoqing Hou*[,§]

*Key Laboratory of Molecular Engineering of Polymers of Ministry of Education, Department of Macromolecular Science, Laboratory of Advanced Materials, Fudan University, Shanghai 200433, People's Republic of China, Institute of Materials Research and Engineering, Agency for Science, Technology and Research (A*STAR), 3 Research Link, Singapore 117602, and College of Chemistry and Chemical Engineering, Jiangxi Normal University, Nanchang 330027, People's Republic of China*

Received: March 19, 2009; Revised Manuscript Received: May 23, 2009

Polyimide (PI) and PI nanocomposite fibers containing different amounts of multiwalled carbon nanotubes (MWNTs) were produced for the first time by electrospinning. The membranes prepared were composed of highly aligned nanofibers and showed significant enhancement in mechanical properties, compared with the membranes prepared by conventional solution-casting method. Surface-functionalized MWNTs were homogeneously dispersed and highly aligned along the fiber axis, whereas most of the pristine MWNTs formed aggregates or bundles and even protruded out of the electrospun nanofibers. The thermal and mechanical properties of polyimide matrix were significantly improved with the incorporation of MWNTs. And the elongation at break of the nanofiber membranes can reach 100% for the nanotube loading level of 3.5 wt %. It was found that electrospinning the in situ prepared MWNT/poly(amic acid) solution can achieve better polymer chain orientation and thus better mechanical properties of the as-prepared membranes. Our study demonstrates a good example for the preparation of high-performance polymer/carbon nanotube nanocomposites by using electrospinning.

1. Introduction

Polyimides (PIs) are a class of representative high-performance polymers possessing the cyclic imide and being usually combined with aromatic groups in the backbone chains. Aromatic polyimides have been extensively investigated due to their excellent thermal stability, mechanical properties, along with their good chemical resistance and dielectric properties. In the past decade, carbon nanotubes (CNTs) based polymer nanocomposites have attracted much attention as CNTs are considered as the ideal reinforcing nanofillers owing to the combination of low density, high aspect ratio, high stiffness, and extremely high strength. Transferring the superior properties of CNTs to polyimide matrix in lightweight and ultrahigh strength nanocomposites can be realized by fabricating PI nanocomposites with uniform carbon nanotube dispersion.[1−6] On the one hand, however, CNTs cannot be effectively dispersed in polymer matrixes because of their high surface area, and the agglomeration usually leads to the deterioration of the properties of materials. On the other hand, it is not easy to achieve alignment of CNTs in the matrixes, which prevents the CNTs from being efficiently used as the ideal reinforcing fillers. Although significant progress in the dispersion of CNTs in polyimide matrix has been made,[3,7,8] alignment of the nanotubes in the matrix still remains a challenge. Usually, the CNT/PI nanocomposites can be fabricated by melt processing,[1,9,10] solution casting,[11] and electrospinning.[5] Among these commonly used approaches, electrospinning has emerged as an effective route for the production of aligned carbon nanotube based nanocomposites.

Electrospinning utilizes an external electrostatic field to generate high surface areas on small fibers with diameters on the nanometer scale and thus is widely used as an effective method to continuously produce polymer nanofibers.[12−19] The electrospun nanofibrous membranes can be used as optical sensors, tissue-engineering scaffolds, nanocomposites, and protective clothing because of their high porosity, high gas permeability, and large surface area per unit mass.[13,20−22] Among these applications, mechanical strength and toughness are extremely important, and one potential avenue for improving the mechanical properties of these membranes is to fabricate CNT/polymer nanofiber membranes. A wide range of polymer/CNT nanocomposite fibers with diameters ranging from several nanometers to several micrometers have been fabricated by electrospinning.[19,13,23−26] However, the nanofibrous polymer nanocomposites produced by electrospinning are usually not as strong or tough as desired due to weak nanofiber interactions, poor CNT dispersion, and the unoptimized orientations for polymer chains and CNTs in the electrospun fibers.

So far, only a few studies have described the preparation of polymer/CNT nanocomposites by electrospinning.[23−26] Delozier et al. fabricated single-walled carbon nanotube (SWNT)/PI nanocomposite fibers by electrospinning.[5] However, there was no significant SWNT alignment in the electrospun nanofibers and the physical properties of the nanofibers and the membranes were not investigated. Until now, there were no reports about the fabrication of multiwalled carbon nanotube (MWNT)/polyimide nanofibers by electrospinning. In this study, neat PI and MWNT/PI nanofibers and the nanofiber membranes with CNT concentrations ranging from 1 to 10 wt % were fabricated by electrospinning. The dispersion and alignment morphologies

* To whom correspondence should be addressed. E-mail: txliu@fudan.edu.cn (T.L.); haoqing@jxnu.edu.cn (H.H.).
[†] Fudan University.
[‡] Agency for Science, Technology and Research.
[§] Jiangxi Normal University.

10.1021/jp9025128 CCC: $40.75
Published on Web 07/01/2009

of MWNTs in the electrospun nanofibers, as well as the thermal and mechanical properties of the nanofiber membranes, were studied in detail.

2. Experimental Section

2.1. Materials. 4,4′-Oxidiphthalic anhydride (ODPA) and 4,4′-oxidianiline (ODA) (Quzhou Kaiyuan Fine Chem. Co.) were purified by sublimation before use. Pristine MWNTs with a diameter range of 5−10 nm were commercially obtained from Chengdu Institute of Organic Chemistry, Chinese Academy of Sciences. The pristine MWNTs were refluxed in concentrated HNO_3 for 12 h with a weight ratio of the acid to the MWNTs of 50:1, thus to remove the impurity of MWNTs and introduce more carboxylic and hydroxyl groups onto the carbon nanotubes.

2.2. Preparation of the Electrospinning Solutions. The precursor of polyimide, poly(amic acid) (PAA) was synthesized from ODPA and ODA with an equivalent molar ratio. The polycondensation was performed in DMAc (N,N-dimethylacetamide) at −3 °C, and the solid content of the pristine PAA solution was 20%. Using an Ubbelodhe viscometer, the inherent viscosity of the prepared PAA solution measured at 25 °C was 2.43 dL g^{-1}. For the preparation of neat PAA solution used for electrospinning, the pristine PAA solution was diluted by DMAc, and for MWNT/PAA solutions, the pristine PAA solution was diluted by MWNT/DMAc solution. As an example, 3.6 g of DMAc or MWNT/DMAc solution was added to 6 g of pristine PAA solution by mechanical stirring at −3 °C for 6 h. Prior to the solution mixing, the MWNT/DMAc solutions were sonicated for 2 h to uniformly disperse the carbon nanotubes. And, the solid content of all the electrospinning solutions was fixed at 12.5 wt %.

The in situ polymerized PAA solution containing 1 wt % functionalized MWNTs was prepared by dispersing MWNTs in DMAc via sonication for 2 h and then in situ synthesizing the MWNT/PAA solution by adding monomers into CNT solution. The solid content of the in situ synthesized MWNT/PAA solution was 15%. As the incorporation of CNTs could hinder the increase of molecular weight of PAA, the solid content of 1 wt % f-MWNT/PAA solution for electrospinning was kept to be 15%, in order to obtain uniform nanofibers free of beads.

2.3. Electrospinning and Imidization. Electrospinning was carried out using a syringe with a spinneret having a diameter of 0.5 mm at an applied voltage of 20−25 kV at ambient temperature. The feeding rate was about 0.25 mL/h, and the spinneret−collector distance was set to be 20 cm. The PAA nanofibers were collected using a rotating disk collector with a diameter of 0.30 m and a width of 8 mm. During electrospinning, the linear speed of the rotating collector was about 24 m s^{-1} because lower rotation speed cannot efficiently align the nanofibers and higher rotation speed usually leads to the breakage of the nanofibers. All the membranes were first dried at 60 °C in vacuum for 5 h to remove the residual solvent and then thermally imidized in N_2 atmosphere using the following program to complete the imidization process: (1) heating up to 150 °C at a rate of 5 °C min^{-1} and annealing for 40 min; (2) heating up to 280 °C at a rate of 2 °C min^{-1} and annealing for 40 min.

2.4. Characterization. Transmission electron microscopy (TEM) observations of nanofibers were performed under an acceleration voltage of 200 kV with a Philips CM 300 FEG TEM. TEM specimens were prepared by directly collecting the electrospun nanofibers onto copper grids during the fabrication of membranes. A scanning electron microscope (SEM, Tescan) was used to observe the surface morphology of the electrospun nanofiber membranes, and SEM was performed at an acceleration voltage of 20 kV. Thermogravimetric analysis (Pyris 1 TGA) was performed under nitrogen flow from 100 to 800 °C at a heating rate of 20 °C min^{-1}. Dynamic mechanical analysis (DMA, Netzsch) of the nanocomposite membranes were carried out under tensile membrane mode from 50 to 300 °C at a frequency of 1 Hz and heating rate of 3 °C min^{-1}. Tensile tests of the nanofiber membranes were carried out on a CMT-8500 electromechanical universal testing machine (SANS), and the samples were directly mounted to the sample clamps and stretched at a speed of 10 mm min^{-1}. Tensile property values reported here represent an average of the results for tests run on at least five samples. Wide-angle X-ray diffraction (WAXD) patterns were recorded with a Bruker GADDS X-ray diffractometer equipped with a two-dimensional (2D) area detector using Cu Kα radiation under a voltage of 40 kV and a current of 40 mA.

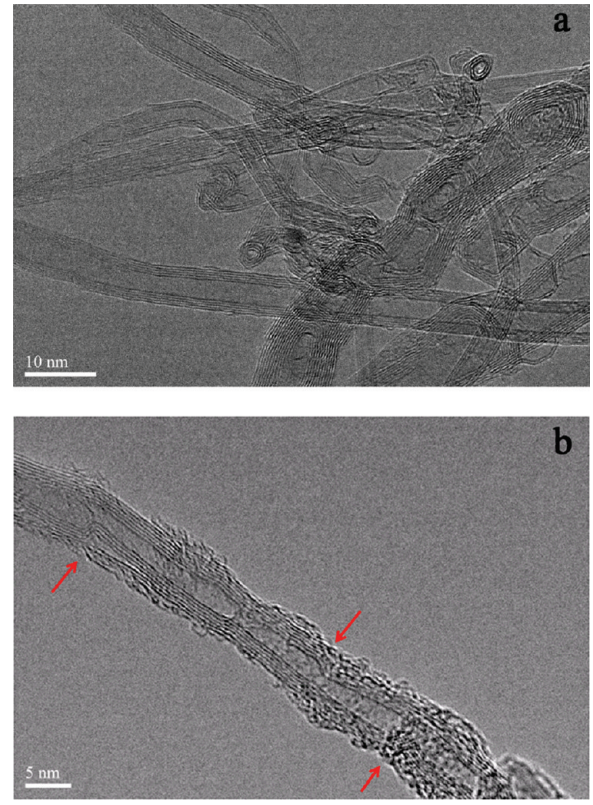

Figure 1. TEM micrographs of (a) p-MWNT and (b) f-MWNT.

3. Results and Discussion

In order to improve the interfacial interaction and compatibility between the MWNTs and the matrix, pristine MWNTs (p-MWNTs) were treated with concentrated HNO_3 to obtain the acid-functionalized MWNTs (f-MWNTs). Figure 1a shows the TEM micrograph of pristine MWNTs with high aspect ratio, and it can be seen that the diameter of the pristine MWNTs with relatively smooth surface were several nanometers to about 10 nm. Figure 1b shows the TEM image of a typical f-MWNT with diameter of about 6−8 nm, and one can clearly see the presence of curvatures or defects (indicated by arrows) on the rough surface of MWNTs after the acid functionalization. To evaluate the functionalization degree of MWNTs, the thermal stability of both p-MWNTs and f-MWNTs was investigated by TGA under nitrogen atmosphere (as shown in Figure 2). The

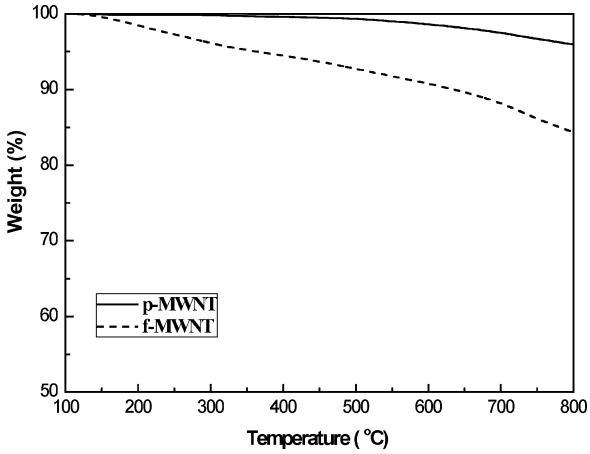

Figure 2. TGA curves of p-MWNT and f-MWNT.

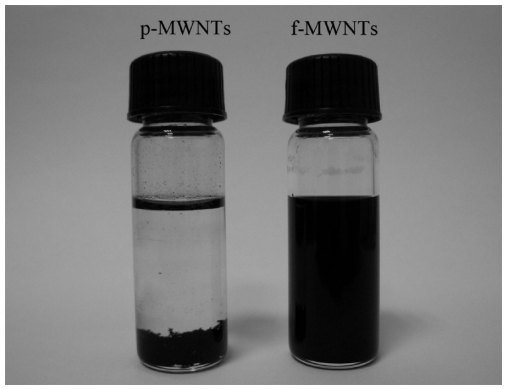

Figure 3. Photographs of p-MWNT and f-MWNT dispersed in DMAc.

TGA results clearly indicated that the MWNTs were highly functionalized (by about 10% at 600 °C) via acid treatment, which was consistent with the TEM observations. Figure 3 shows the typical photographs of the DMAc solutions of p-MWNTs and f-MWNTs after being sonicated for 1 h and then stored for 2 months. It indicates that the f-MWNTs can be stably dispersed in DMAc due to the introduction of carboxyl or hydroxyl groups to the MWNT surfaces. However, the DMAc solution of p-MWNTs is not stable and the CNTs are deposited at the bottle bottom only after a few days.

It is known that the diameter uniformity and absence of beads in the electrospun nanofibers are of vital importance for fabricating membranes with good mechanical properties. As the polymer solution properties (viscosity, surface tension, etc.) and electrospinning conditions (voltage, spinneret−collector distance, etc.) greatly influence the morphology of the electrospun nanofibers, we made first efforts to optimize the electrospinning conditions by changing these experimental parameters. In the present work, the average diameter of the nanofibers was controlled in the range of 200−300 nm to ensure the uniformity of the electrospun nanofibers. In order to eliminate the influence of molecular weight on the mechanical properties of the nanofiber membranes and investigate how the CNT incorporation influences the properties of electrospun membranes, the electrospinning solutions with different CNT loadings (0−10 wt %) were prepared by mixing pristine PAA solution with DMAc or CNT/DMAc solutions.

Usually, the electrospun nanofibers were spun onto a stationary plate collector, thus resulting in membranes or mats that consist of randomly arranged fibers. As the nanofibers were collected in nonwoven sheets and the interactions between the nanofibers were very weak, the nanofibers could be easily slipped or pulled out from each other, and therefore, nanofiber membranes collected by this method usually possess poor mechanical properties. In this study, a high-speed rotating collector (as shown in Figure 4) was used to fabricate neat PI and MWNT/PI membranes.

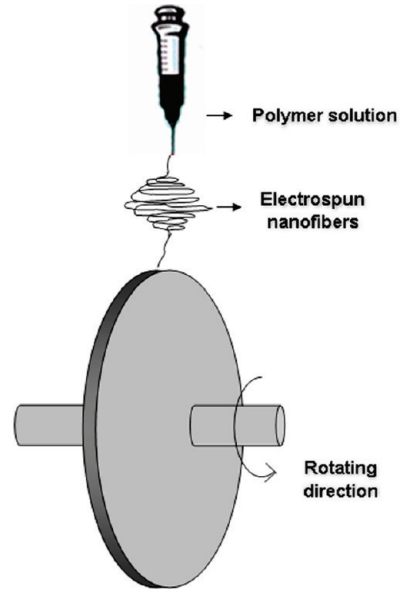

Figure 4. Schematic of the electrospinning process equipped with a rotating collector.

In order to demonstrate the high-speed rotation collecting method can produce membranes with highly aligned electrospun nanofibers, neat PAA nanofibers were also collected on a stationary aluminum foil for comparison. As shown in Figure 3, the membrane collected without using the rotating collector consisted of randomly oriented nanofibers (Figure 5a), whereas the nanofibers collected by high-speed rotating method were highly aligned (Figure 5b). The SEM photograph of aligned neat PI nanofiber membrane at a higher magnification is shown in Figure 5c. It can be seen that the surfaces of the electrospun nanofibers were smooth and almost free of defects such as beads. During the electrospinning process, the rotating collector was connected to a negative electrode (about −5 kV) in order to control the placement and alignment of the fibers, and the nanofibers would track the electrical field lines and attach to the negatively charged rotating collector.[13] Some nanofibers were entangled and could not be differentiated or separated individually (as shown in Figure 5c), probably because the fast jet of the nanofibers and the traction of the rotating collector make some of the nanofibers contacted and entangled with each other during the electrospinning. In addition, the nanofibers may be partially fused during the (subsequent) high-temperature imidization process, and this may also lead to the entanglement of the nanofibers.

Besides neat PAA, PAA nanofiber membranes containing pristine and acid-modified MWNTs were also fabricated by electrospinning. During the electrospinning process, some nanofibers were collected on copper grids for TEM observations. As shown in TEM image of Figure 6a, p-MWNTs were mostly agglomerated and could not be well dispersed in PAA matrix. The entangled nanotubes were prone to aggregate close to the nanofiber surface rather than being aligned well in the nanofibers, thus leading to the coarseness of surface and the ununiformity of the diameters of the electrospun nanofibers.

Figure 6b shows the TEM micrograph (at low magnification) of PAA nanofibers with 2 wt % f-MWNTs. It can be seen that

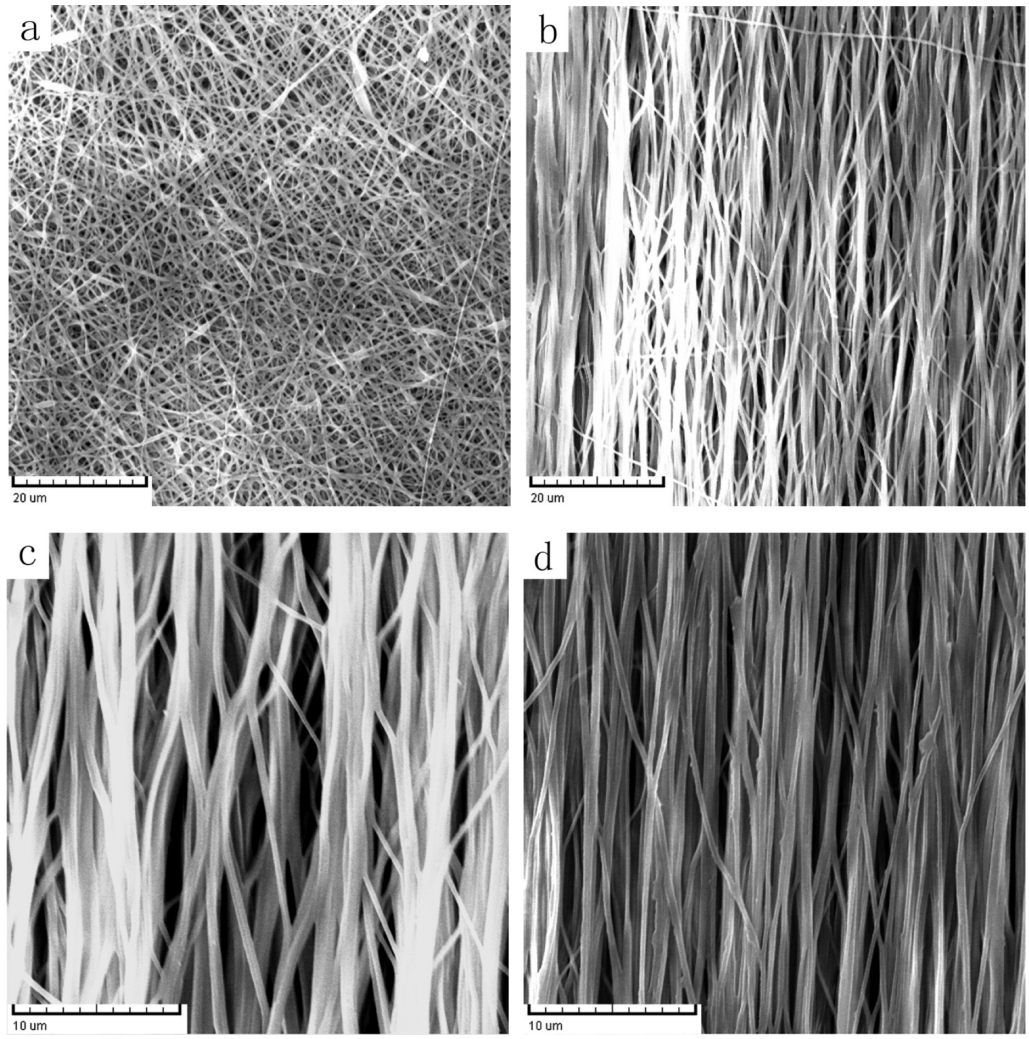

Figure 5. SEM micrographs of neat polyimide membranes consisting of (a) nonaligned nanofibers; (b) aligned nanofibers under low magnification; (c) aligned nanofibers under high magnification; (d) aligned nanofibers after tensile tests.

the surfaces of nanofibers were smooth, and no beads or other defects were observed in the nanofibers. Figure 6c shows a TEM micrograph at high magnification for PAA nanofibers with 2 wt % f-MWNTs. It was clearly seen that most of the carbon nanotubes were well dispersed and highly aligned along the nanofiber axis. Therefore, chemical functionalization of MWNTs can greatly improve their dispersion and orientation within the PAA nanofibers, especially at low carbon nanotube concentration. Figure 6d shows the TEM micrograph of PAA nanofibers containing 7.5 wt % f-MWNTs. Although some CNTs are slightly folded or aggregated in the nanofiber, generally speaking, homogeneous dispersion and high orientation of MWNTs can be still achieved even at this high nanotube loading level. When further increasing the MWNT concentration (e.g., 10 wt %), the carbon nanotubes tended to form bundles or agglomerations within the electrospun nanofibers significantly (Figure 6e).

It should be noted that one interesting phenomenon was always observed for the electrospun PAA/CNT nanofibers: most of the pristine MWNT bundles were preferably located close to the nanofiber surfaces or even protruded out of the nanofiber surface (Figure 6a), whereas the functionalized MWNTs could be easily dispersed and thus uniformly distributed over the whole nanofibers. It was also reported that the entangled or knotted nanotubes were protruded out of the polycaprolactone nanofibers.[25] We suspected that this phenomenon could be attributed to the high surface energy of the pristine MWNTs which were inclined to be entangled or agglomerated and protruded out of the nanofiber surface thus to reduce their surface energy. After surface modification, however, the surface energy of the functionalized MWNTs decreased significantly, and thus almost no agglomerations or protrusions were observed in the PAA nanofibers (Figure 6, parts b and c). And, with further increasing the f-MWNT content, even the functionalized CNTs have a tendency to be aggregated and thus are preferably located in the region close to the nanofiber surfaces. Such a phenomenon was occasionally observed in the cases with high CNT loading levels, such as 7.5 and 10 wt % f-MWNTs (Figure 6, parts d and e).

In this study, the high degree of CNT alignment along the PAA nanofibers can be attributed to the successful functionalization of the MWNTs and appropriate adjusting of the electrospinning conditions. Several factors may contribute to the high alignment of MWNTs along the electrospun PAA nanofibers: (1) large electrostatic fields and the shear forces present in the liquid jet during electrospinning; (2) the so-called nanoscale confinement effect. There are not many permissible orientations for carbon nanotubes in the electrospun nanofibers because of the large aspect ratio of the nanotubes and the nanoscale diameter of the electrospun nanofibers;[27] (3) the movement and orientation of PAA chains during electrospinning will also be beneficial to the alignment of carbon nanotubes due to the interactions between the acid-modified CNTs and PAA chains.

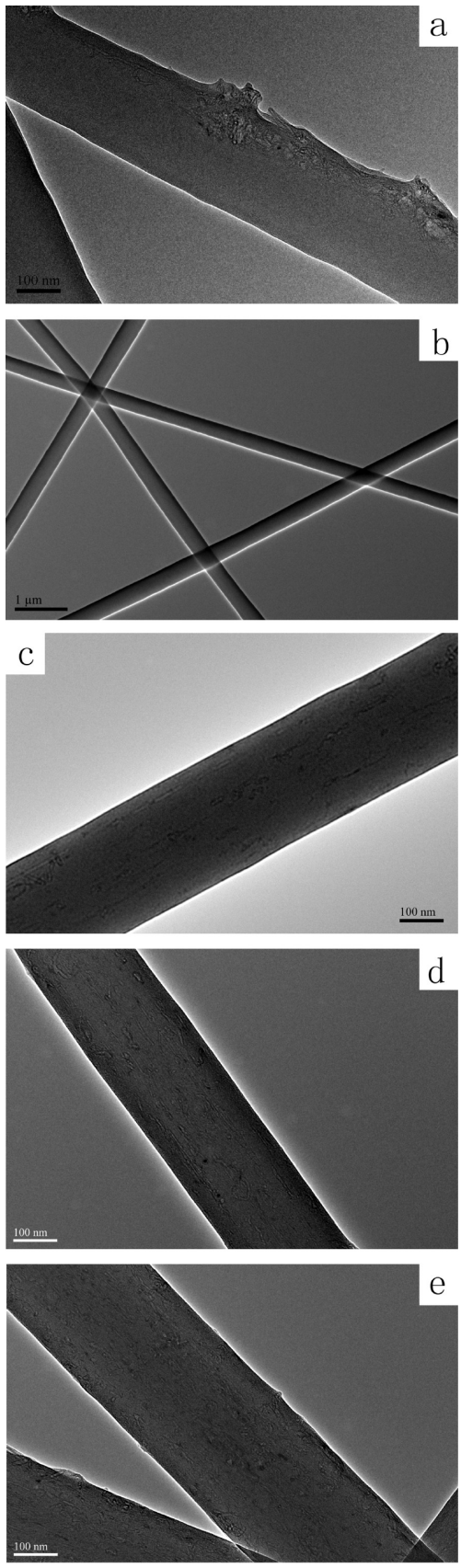

Figure 6. TEM micrographs of PAA nanofibers containing (a) 1 wt % p-MWNTs, (b) 2 wt % f-MWNTs (at low magnification), (c) 2 wt % f-MWNTs (at high magnification), (d) 7.5 wt % f-MWNTs, and (e) 10 wt % f-MWNTs.

Therefore, a coupling effect of the above factors leads to a preferred alignment of MWNTs along the electrospun PAA nanofibers.

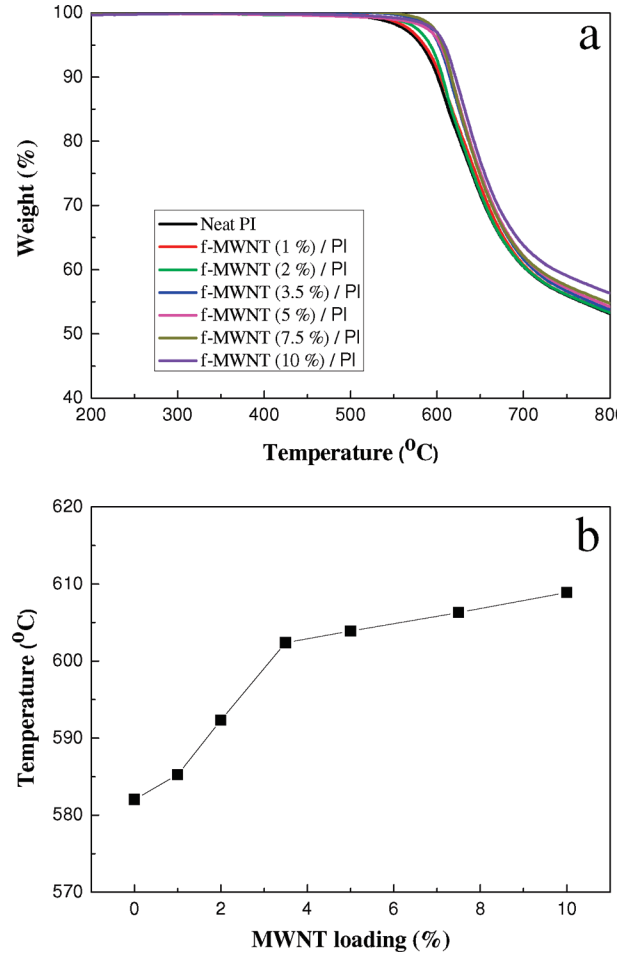

Figure 7. (a) TGA curves of neat PI and its nanofiber membranes as a function of f-MWNT content; (b) 5% weight loss temperature vs f-MWNT content of the electrospun nanofiber membranes.

From the above results, it can be concluded that the fine dispersion of carbon nanotubes is of vital importance for their alignment within the electrospun nanofibers. When being effectively debundled and well dispersed in the matrix, MWNTs can be easily aligned in the polymer nanofibers by electrospinning. Clearly, chemical functionalization and physical dispersion method such as sonication treatment can significantly improve the dispersion of MWNTs. However, some MWNTs are definitely damaged or broken upon such treatments, and defects and fragments of CNTs can be occasionally seen from the TEM micrographs of the f-MWNT and the f-MWNT/PAA nanofibers, which will somewhat deteriorate the performance of the electrospun nanofibers. Therefore, how to efficiently modify the carbon nanotubes without destroying their surface morphology and achieve their homogeneous dispersion and high alignment is still a great challenge.

Carbon nanotubes are usually used to enhance the thermal stability of polymer materials because of their inertness to thermal treatment. Figure 7a shows the TGA curves under nitrogen atmosphere for neat PI and MWNT/PI nanofiber membranes. It can be seen that all the electrospun nanofibers possess excellent thermal stability and the residual weights of the membranes increase with the increase of CNT content. As shown in Figure 7b, with increasing the MWNT concentration, the 5% weight loss temperature (T_d) increased gradually. Upon incorporation of only 3.5 wt % CNT, the 5% weight loss temperature (i.e., thermal stability) of PI membranes is significantly improved by about 20 °C, due to the fine dispersion of

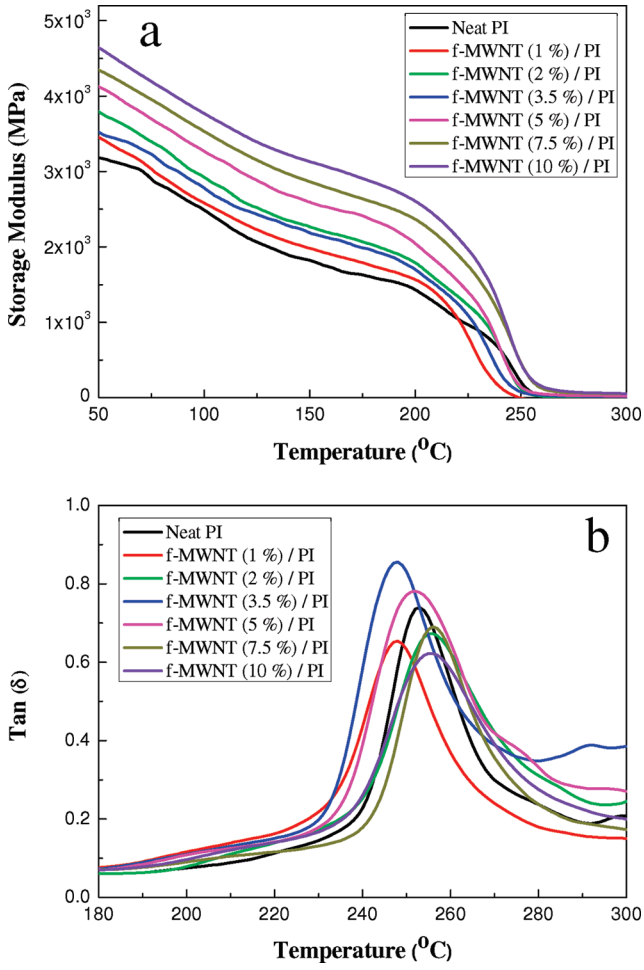

Figure 8. DMA curves of (a) storage modulus (G') and (b) tan(δ) vs temperature for neat PI and PI/CNT nanofiber membranes.

high aspect ratio MWNTs in the matrix. For the cases of CNT loading level above 3.5 wt %, the increasing trend of the T_d slightly decreases, probably indicating the occurrence of some CNT agglomerations. When the CNT content is up to 10 wt %, the decomposition temperature is enhanced by about 30 °C. There are two competing factors during the decomposition of PI composites. On the one hand, the chemical functionalization can remove the impurity of MWNTs and assist the fine dispersion of nanotubes in the matrix thus improving the thermal stability of materials. On the other hand, however, the carboxyl or hydroxyl groups introduced into the MWNTs are easily decomposed at high temperature and may deteriorate the thermal stability of PI matrix. Hence, excessive destruction of the surface nanostructure of carbon nanotubes by chemical modifications (in order to achieve fine nanotube dispersion) would not play a positive role in the improvement of certain physical properties such as thermal stability of the nanocomposites.

Parts a and b of Figure 8 depict the DMA results showing storage modulus (G') and tan(δ) versus temperature curves for neat PI and its CNT nanofiber membranes. The moduli of nanofiber membranes steadily increased with the concentration of MWNTs (Figure 8a). However, the change of T_g (glass transition temperature) did not show any trend. We suspect the complex and variable changes of T_g may be attributed to the following reasons: (1) the difference or variation in polyimide chain orientation in the electrospun nanofibers (as the T_g reflects the chain mobility or constraints), (2) the presence of micro-defects in the nanofibers and the membranes, and (3) the experimental errors brought about during the DMA measurements.

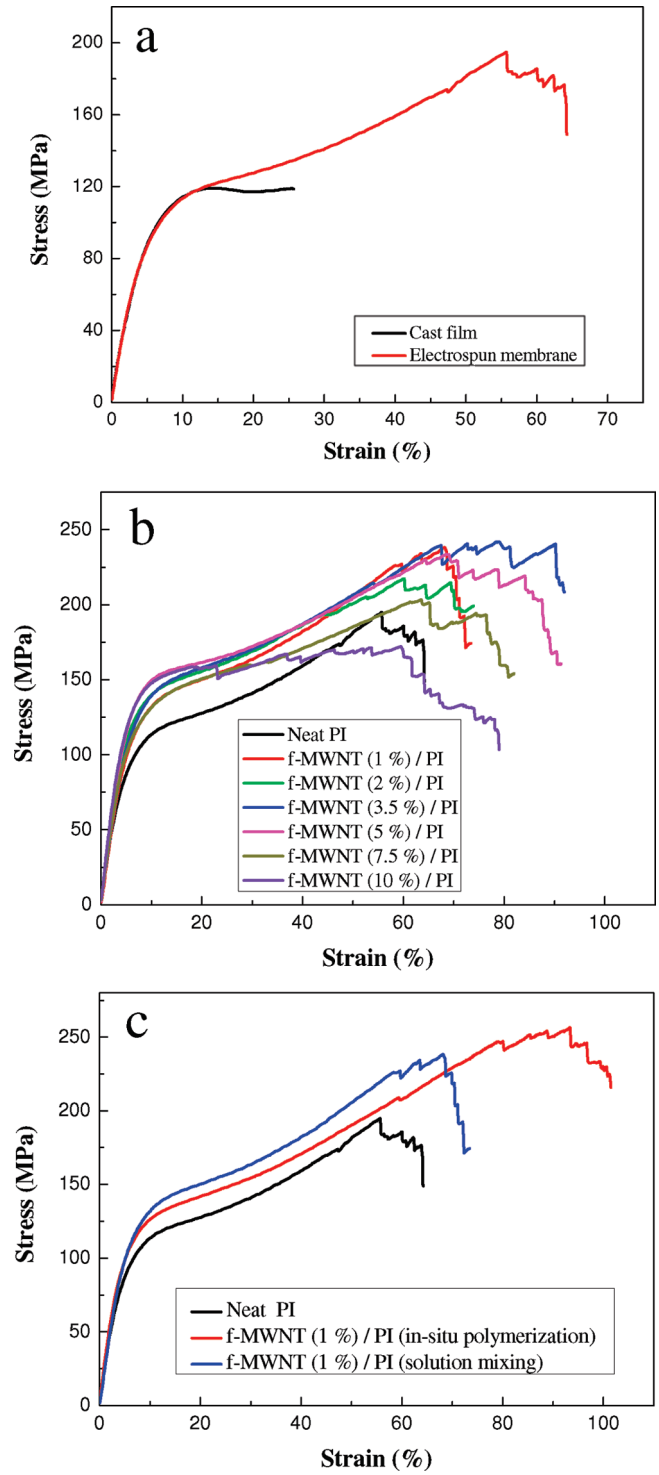

Figure 9. Stress−strain curves for (a) neat PI membranes prepared by casting and electrospinning; (b) neat PI and f-MWNT/PI nanofiber membranes with different CNT contents; (c) neat PI, 1 wt % f-MWNT/PI nanofiber membranes fabricated by electrospinning of solution-mixed and in situ polymerized MWNT/PAA solutions.

To compare the mechanical properties of aligned nanofiber membranes with those of the conventional solution-cast film, neat PI films were also prepared by directly casting on glass plates. The representative stress−strain curves of neat PI membranes prepared by casting and electrospinning are shown in Figure 9a. Although the tensile modulus and yield strength of neat PI membranes prepared by casting and electrospinning were nearly the same, the tensile strength and elongation at break (or toughness) of electrospun membrane were much higher than

TABLE 1: Summary of Mechanical Properties of the Electrospun Neat PI and Its Nanofiber Membranes As a Function of f-MWNT Concentration

sample	yield strength (MPa)	tensile strength (MPa)	tensile modulus (GPa)	elongation at break (%)
neat PI nanofiber membrane	128.2 ± 15	186.8 ± 20	2.47 ± 0.34	64.1 ± 10
f-MWNT (1%)/PI	170.7 ± 20	206.1 ± 30	2.67 ± 0.23	73.1 ± 16
f-MWNT (2%)/PI	175.3 ± 20	214.7 ± 15	2.78 ± 0.13	73.8 ± 8.0
f-MWNT (3.5%)/PI	200.9 ± 16	239.7 ± 21	2.56 ± 0.15	90.5 ± 11
f-MWNT (5%)/PI	176.5 ± 31	223.4 ± 17	2.99 ± 0.31	89.9 ± 24
f-MWNT (7.5%)/PI	164.6 ± 25	199.5 ± 16	2.71 ± 0.30	86.9 ± 14
f-MWNT (10%)/PI	144.3 ± 30	168.4 ± 30	3.12 ± 0.21	71.2 ± 30

those of the cast film, due to the high orientation of the electrospun nanofibers in the membranes. A steady increase or hardening of the stress after the yield point for the electrospun membrane was observed. However, this was not seen for the cast film. As shown in Figure 5c, not all the nanofibers in the electrospun membranes were highly aligned along the rotation direction. At the early stage of the tensile tests, only some nanofibers may work and bear the load. And during the tensile testing, most nanofibers in the membrane are extended and suffered the load thus leading to a steady increase of tensile strength and an enhanced toughness. Figure 5d shows the surface morphology of neat PI membrane after tensile testing. It can be seen that the nanofibers after the tensile test were aligned better along the rotation direction and became much dense than the as-prepared electrospun membranes (Figure 5c).

Figure 9b shows the typical stress−strain curves of neat PI and PI nanofiber membranes with different contents of f-MWNTs. The average tensile properties such as yield and tensile strengths, tensile modulus, and elongation at break are summarized in Table 1. It can be seen that all the electrospun membranes display a linear elastic deformation at low strain (<8%) followed by a plastic deformation up to failure. Generally, adding a small amount of carbon nanotubes (e.g., 1 wt %) can dramatically improve the overall tensile properties of polyimide membranes. With the increase of CNT content, the modulus of the membranes increased, and the 10 wt % CNT/PI membrane possessed the highest tensile modulus among the systems studied here. However, the optimized tensile or yield strength was observed for the membrane containing 3.5 wt % f-MWNTs, and elongation at break can reach nearly 100%. When further increasing the CNT concentration (from 3.5 to 10 wt %), all the values of the tensile or yield strength and elongation at break began to gradually decrease. And for the membrane containing 10 wt % MWNTs, its tensile strength was even lower than neat PI membrane. Therefore, the tensile results may indicate again that CNT agglomerations are probably formed to certain extent when the CNT concentration is above 3.5 wt %. As is known, polyimide is one kind of ultrastrong polymer and usually possesses low toughness or elongation at break. Here, high-performance polyimide nanocomposites were successfully fabricated with high toughness and enhanced overall mechanical properties by incorporation of carbon nanotubes.

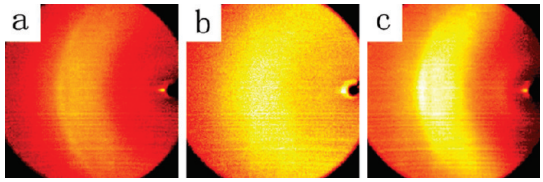

Figure 10. Two-dimensional WAXD patterns of electrospun (a) neat PI membrane and 1 wt % MWNT/PI nanofiber membranes fabricated by electrospinning of (b) solution-mixed and (c) in situ polymerized MWNT/PAA solutions.

As carbon nanotubes cannot be easily dispersed in polymer matrix, in situ polymerization was usually employed to fabricate polymer nanocomposites with homogeneous nanotube dispersion. In order to investigate whether PI nanocomposites with better CNT dispersion can be obtained via in situ polymerization, 1 wt % f-MWNT/PI nanofiber membrane was also fabricated by electrospinning of in situ polymerized MWNT/PAA solution, compared with the case of the above electrospinning MWNT/PAA solutions prepared by solution mixing. The stress−strain curves of neat PI nanofiber membrane and the ones containing with 1 wt % f-MWNTs are shown in Figure 9c. It can be seen that the tensile strength and toughness of 1 wt % f-MWNT/PI nanofiber membrane prepared by in situ polymerization were slightly higher than that by solution mixing. However, the dispersion morphology of MWNTs did not show much difference between the above two methods. Hence, the nanofiber membranes were investigated by using WAXD. The 2D WAXD patterns obtained from the above electrospun membranes are shown in Figure 10a−c, respectively. It can be seen that the in situ polymerized CNT/PI membranes possess much brighter reflection arcs and much sharper or clearer edges. This indicates that the in situ polymerization method (Figure 10c) can fabricate nanofiber membranes with higher chain orientation than the solution mixing method. Higher orientation of polyimide chains may be probably associated with the interactions between the polymer chains and carbon nanotubes. During the in situ polymerization, the CNTs may be first dispersed in DMAc solution and interact with monomers. The polymer chains are formed thereafter, thus resulting in better CNT/PAA interactions and higher orientation of polymer chains. Therefore, higher orientation of polymer chains may lead to better mechanical property of in situ polymerized MWNT/PI membranes. The exact reasons for this phenomenon need to be further investigated.

4. Conclusion

In this contribution, high-performance polyimide nanofiber membranes containing carbon nanotubes have been developed by an electrospinning technique. All the electrospun nanofibers were highly aligned along the collector rotation direction. TEM micrographs indicated that the functionalized MWNTs were homogeneously dispersed in polyimide matrix, whereas the unmodified MWNTs were agglomerated and protruded out of the nanofiber surfaces. The thermal and mechanical properties of polyimide membranes were improved by the incorporation of carbon nanotubes. The elongation at break of nanofiber membranes can reach 100% for the nanotube loading level of 3.5 wt %. Two-dimensional WAXD results showed that electrospinning of the in situ polymerized CNT/PAA solution is an efficient way to improve polyimide chain orientation and thus achieve the membranes with better tensile strength and toughness. Such fabrication of high-performance PI/CNT nanofiber membranes is an important step toward utilizing carbon nanotubes in polymer matrixes to achieve ultrastrong, tough,

and lightweight nanocomposites that can be used in defense or aerospace areas.

Acknowledgment. This work was supported by the National Natural Science Foundation of China (20774019, 50873027), the Program for Changjiang Scholars and Innovative Research Team in University (PCSIRT) (project no. IRT0612), and the Shanghai Leading Academic Discipline Project (project no. B113).

References and Notes

(1) Siochi, E. J.; Working, D. C.; Park, C.; Lillehei, P. T.; Rouse, J. H.; Topping, C. C.; Bhattacharyya, A. R.; Kumar, S. *Composites, Part B: Eng.* **2004**, *35*, 439.

(2) Smith, J. G.; Delozier, D. M.; Connell, J. W.; Watson, K. A. *Polymer* **2004**, *45*, 6133.

(3) Jiang, X. W.; Bin, Y. Z.; Matsuo, M. *Polymer* **2005**, *46*, 7418.

(4) Delozier, D. M.; Watson, K. A.; Smith, J. G.; Connell, J. W. *Compos. Sci. Technol.* **2005**, *65*, 749.

(5) Delozier, D. M.; Watson, K. A.; Smith, J. G.; Clancy, T. C.; Connell, J. W. *Macromolecules* **2006**, *39*, 1731.

(6) Yu, A. P.; Hui, H.; Bekyarova, E.; Itkis, M. E.; Gao, J.; Zhao, B.; Haddon, R. C. *Compos. Sci. Technol.* **2006**, *66*, 1190.

(7) Qu, L. W.; Lin, Y.; Hill, D. E.; Zhou, B.; Wang, W.; Sun, X. F.; Kitaygorodskiy, A.; Suarez, M.; Connell, J. W.; Allard, L. F.; Sun, Y. P. *Macromolecules* **2004**, *37*, 6055.

(8) Yuen, S. M.; Ma, C. C. M.; Chiang, C. L.; Lin, Y. Y.; Teng, C. C. *J. Polym. Sci., Part A: Polym. Chem.* **2007**, *45*, 3349.

(9) Ogasawara, T.; Ishida, Y.; Ishikawa, T.; Yokota, R. *Composites, Part A: Appl. Sci.* **2004**, *35*, 67.

(10) Ghose, S.; Watson, K. A.; Sun, K. J.; Criss, J. M.; Siochi, E. J.; Connell, J. W. *Compos. Sci. Technol.* **2006**, *66*, 1995.

(11) Zhou, B.; Lin, Y.; Hill, D. E.; Wang, W.; Veca, L. M.; Qu, L. W.; Pathak, P.; Meziani, M. J.; Diaz, J.; Connell, J. W.; Watson, K. A.; Allard, L. F.; Sun, Y. P. *Polymer* **2006**, *47*, 5323.

(12) Xuyen, N. T.; Ra, E. J.; Geng, H. Z.; Kim, K. K.; An, K. H.; Lee, Y. H. *J. Phys. Chem. B* **2007**, *111*, 11350.

(13) Carnell, L. S.; Siochi, E. J.; Holloway, N. M.; Stephens, R. M.; Rhim, C.; Niklason, L. E.; Clark, R. L. *Macromolecules* **2008**, *41*, 5345.

(14) Hou, H. Q.; Ge, J. J.; Zeng, J.; Li, Q.; Reneker, D. H.; Greiner, A.; Cheng, S. Z. D. *Chem. Mater.* **2005**, *17*, 967.

(15) Jaeger, R.; Schonherr, H.; Vancso, G. J. *Macromolecules* **1996**, *29*, 7634.

(16) Reneker, D. H.; Chun, I. *Nanotechnology* **1996**, *7*, 216.

(17) Reneker, D. H.; Yarin, A. L.; Fong, H.; Koombhongse, S. *J. Appl. Phys.* **2000**, *87*, 4531.

(18) Fong, H.; Chun, I.; Reneker, D. H. *Polymer* **1999**, *40*, 4585.

(19) Ge, J. J.; Hou, H. Q.; Li, Q.; Graham, M. J.; Greiner, A.; Reneker, D. H.; Harris, F. W.; Cheng, S. Z. D. *J. Am. Chem. Soc.* **2004**, *126*, 15754.

(20) Johnson, J.; Ghosh, A.; Lannutti, J. *J. Appl. Polym. Sci.* **2007**, *104*, 2919.

(21) Sundarrajan, S.; Ramakrishna, S. *J. Mater. Sci.* **2007**, *42*, 8400.

(22) Bergshoef, M. M.; Vancso, G. J. *Adv. Mater.* **1999**, *11*, 1362.

(23) Pan, C.; Ge, L. Q.; Gu, Z. Z. *Compos. Sci. Technol.* **2007**, *67*, 3271.

(24) Vaisman, L.; Wachtel, E.; Wagner, H. D.; Marom, G. *Polymer* **2007**, *48*, 6843.

(25) Saeed, K.; Park, S. Y.; Lee, H. J.; Baek, J. B.; Huh, W. S. *Polymer* **2006**, *47*, 8019.

(26) Blond, D.; Walshe, W.; Young, K.; Blighe, F. M.; Khan, U.; Almecija, D.; Carpenter, L.; McCauley, J.; Blau, W. J.; Coleman, J. N. *Adv. Funct. Mater.* **2008**, *18*, 2618.

(27) Ayutsede, J.; Gandhi, M.; Sukigara, S.; Ye, H. H.; Hsu, C. M.; Gogotsi, Y.; Ko, F. *Biomacromolecules* **2006**, *7*, 208.

JP9025128